

In consideration of precursor states, spillover and Boudart's 'collection zone' and of their role in catalytic processes

M. Bowker*, L.J. Bowker, R.A. Bennett, P. Stone, A. Ramirez-Cuesta

Department of Chemistry, Centre for Surface Science and Catalysis, University of Reading, Reading RG6 6AD, UK

Received 23 February 2000; accepted 5 June 2000

Abstract

Various aspects of 'spillover' and 'reverse spillover' in catalysis are considered. The ideas of Kisliuk regarding the kinetic role of weakly held adsorbed states as precursors to stronger chemisorption are shown to be important for reverse spillover, as highlighted by Boudart's concept of the 'collection zone'. STM has proved to be an important tool for the understanding of the formation and thermal evolution of nanoparticles on surfaces. Here we present direct, in situ observations of spillover for the reaction of oxygen with Pd nanoparticles on TiO₂(1 1 0). In turn, this is connected to a form of SMSI, and it is proposed that this spillover may also be the mechanism of the oxygen storage phenomenon for CeO₂-doped automobile catalysts. © 2000 Elsevier Science B.V. All rights reserved.

Keywords: Collection zone; Spillover; Boudart; Oxygen storage; SMSI; Catalysis; Nanoparticles; STM

1. Introduction

In recent years, surface science studies related to catalysis have advanced from single crystal work to the fabrication of model nanoparticulate catalysts (for reviews, see [1] and [20]). In some ways these bridge the materials gap perceived to exist between bulk samples (single crystals, for example) and industrial catalysts. This is important in the context of catalysis since, as shown in Fig. 1, it is possible that very small particles do not behave like single crystals for a variety of reasons. These include the fact that if the particle is very small (say <2 nm), the average surface co-ordination is very low (surface energy is high). Also, there are so few atoms in the particle that a metallic-like conduction band is not formed because there is not a 'continuum' of energy levels. The equation in Fig. 1

gives an approximate relationship between the number of atoms in a particle and the spacing of energy levels in the particle, and is related to the Fermi energy of the metal. Thus, a 2 nm hemispherical particle (which will consist of approximately $n = 120$ atoms), with a typical metal work function of 4.5 eV, will have levels spaced by approximately 4 kJ mol⁻¹. However, a particle of half that size has a spacing of around 30 kJ mol⁻¹, making electron conduction highly activated and difficult at room temperature.

Additional factors, which may modify small particle behaviour, include the possibilities of spillover, that is diffusion of reactive species from the metal to the support or vice-versa (reverse spillover). This can include diffusion of inorganic oxides from the support onto the metal, the proposed source of the SMSI effect in catalysis. Such diffusion effects are of limited range and are, therefore, likely to be of greatest significance for the behaviour of small particles. Also the particle-support interface may be the location of the

* Corresponding author.

E-mail address: m.bowker@rdg.ac.uk (M. Bowker).

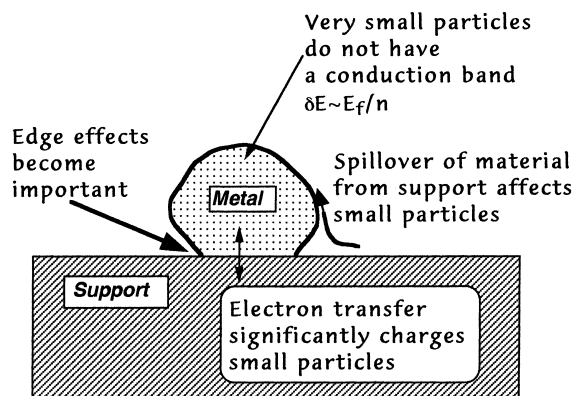


Fig. 1. A model of a supported metal particle, illustrating possible reasons why it can be different in behaviour when compared with that of a bulk metal sample.

active site for some types of reaction; for small particles there are more such active sites per unit weight of metal loaded. Finally, in the context of this figure, charge transfer can take place between the support and the metal, and this is likely to have the biggest effect on the electronic structure and reactivity of the smallest particles.

Early work on nanoparticulate model catalysts has largely concentrated on fabrication and the physical properties of such materials, and measurements of their reactivity has only recently begun [2]. It is of crucial importance to the future of this field of study that detailed measurements begin to be made of sticking probabilities and of their dependence on uptake. Such measurements can be directly compared with single crystal results to determine the effect of the dimensionality change. It is further important in relation to understanding metal-support effects in catalysis. The theme of the current paper is to describe some ideas and initial findings regarding the nature of the interaction between nanoparticles and the support, especially as determined by using high resolution scanning tunnelling microscopy carried out in the author's group. This is particularly relevant in the case of this special publication since Boudart's work at Princeton and Stanford has highlighted the importance of the diffusion of molecules between an (apparently) unreactive support and an active metal phase; some of this work is outlined further in Section 3 below. This area of work is an expanding one in surface science and

will become a major field of endeavour for scientists working on fundamental properties of surfaces in the new millennium.

2. Making and imaging nanoparticles

In the images shown in Fig. 2 the nanoparticles were formed by metal vapour deposition (MVD). In general, Auger electron spectroscopy or XPS can be used, at least approximately, to determine the surface coverage by metal. When the coverage is high, a porous metal film is formed and annealing this then produces nanoparticles as seen in Fig. 2. Of course, a variety of other methods can be used to form particles, including MOCVD (reaction of metal-organic compounds with the surface) and wet preparation methods. These latter methods can present problems with obtaining pure, uncontaminated nanoparticulate surfaces, whereas MVD appears to be a very successful method in this respect.

We need to ask ourselves the question in reference to such work, what is it that we are imaging — is the tip imaging the nanoparticle, or is the nanoparticle (which can have similar dimensions to an STM tip) imaging the tip? We can carry out simple modelling of the imaging process to make some estimates about the nature of this tip–surface interaction. If we imagine, for simplicity, a hemispherical tip approaching a hemispherical particle, the geometrical situation is as shown in Fig. 3a. Tunnelling between the tip and the particle occurs at a certain point, and at that point the feedback system will begin to apply a voltage to the z -piezo driver to raise the tip from the surface and it will then follow the profile of the particle. In order to trace the profile measured in a line scan we need to define the x and z positions of the tip, and these derive from the geometry in Fig. 3a. From that figure it is clear that

$$\sin \theta = \frac{(R+z)}{(R+r)} \text{ and so } z = (R+r)\sin \theta - R \quad (1)$$

and

$$\cos \theta = \frac{x}{(R+r)} \text{ and so } x = (R+r)\cos \theta \quad (2)$$

When $\theta = 90$, then $nz = r$, and so, in general, the height of the particle is measured well, but outside

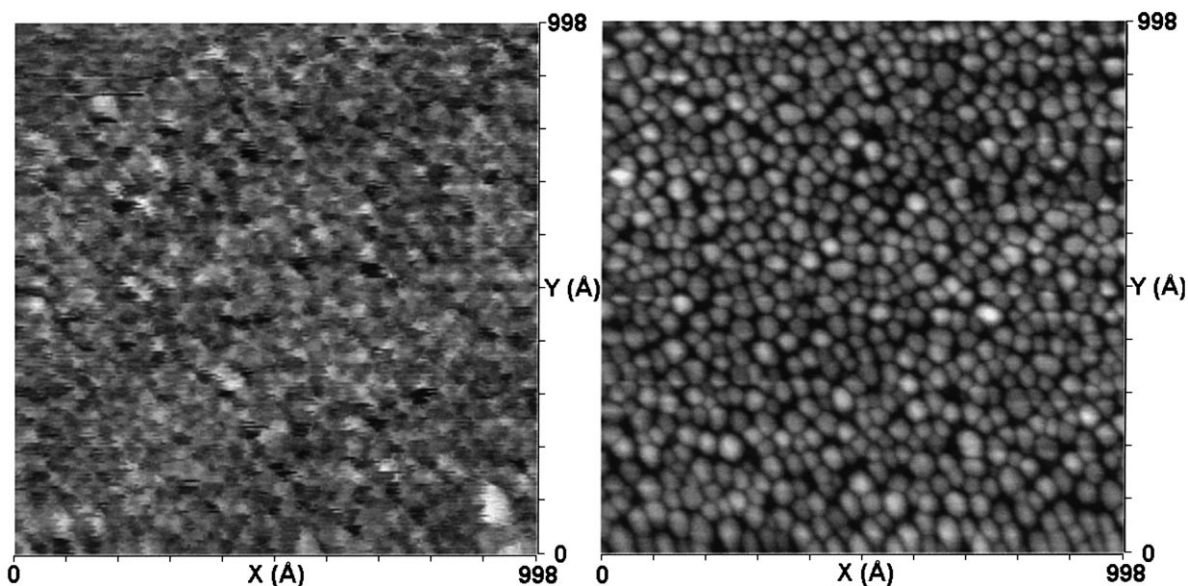


Fig. 2. STM images of an as-deposited Pd film (left image, 1.7 monolayers Pd) at 300 K and that film annealed to 473 K for 15 min (right image), showing an array of nanoparticles with an average size of around 4 nm. Tunnelling conditions were 1 nA, 2 V. The support was TiO_2 (1 1 0).

this the shape depends on both tip and particle shape.

Thus, as shown in Fig. 3, if the tip radius is small compared to the particle, then the particle is imaged (as might be expected), whereas for the reverse situation the tip is imaged. Note that here this has little to do with whether there is a single atom at the apex of the tip because as the tip traverses a nanoparticle its own shape is probed. In all cases, of course, the particle is enlarged in the image by convolution with the tip shape, but this is minimised with big nanoparticles and a small radius tip. In all cases, the tip does well at determining the particle height, but care has to be taken in determining particle size distributions for small particles. Even if a small particle were hemispherical, it will generally be imaged as a flattened particle, and certainly the wetting angle is difficult to determine accurately.

Fig. 4a shows an example of the imaging of an individual particle of well-defined shape. This particle is apparently a ziggurat shape with facets exposed having steps within them. The top plane here is probably (1 0 0) and the sides stepped (1 1 1), as modelled in Fig. 4b. The ability to image some details of the structure in Fig. 4a shows that the tip size is relatively

small. Using a model as in Fig. 4b, and a geometric model appropriate for a ziggurat, an estimate of the tip radius in this case is 3 nm, although the particle itself may not be as ordered and well-defined as is shown in Fig. 4b.

In general, there has been little success in obtaining atomic resolution on small particles, but there are some notable exceptions to this, albeit for very special samples [3,4]. Thus, Henry has given some indication of atomic resolution on small particles of Pd on MoS_2 which were two layers thick [3], while Hojrup Hansen et al. have imaged very thin Pd particles of large lateral dimensions on a special type of alumina film [4].

The imaging of small nanoparticles using scanning probe microscopy (SPM) is very important since it represents an analytical tool for the investigation of important properties of catalysts, such as sintering, faceting, spillover, redispersion, etc. These may not be amenable to study on high area porous materials. Surface diffusion of various types is implicated in these processes, and the importance of surface diffusion for the reactivity of catalysts is highlighted in the following sections.

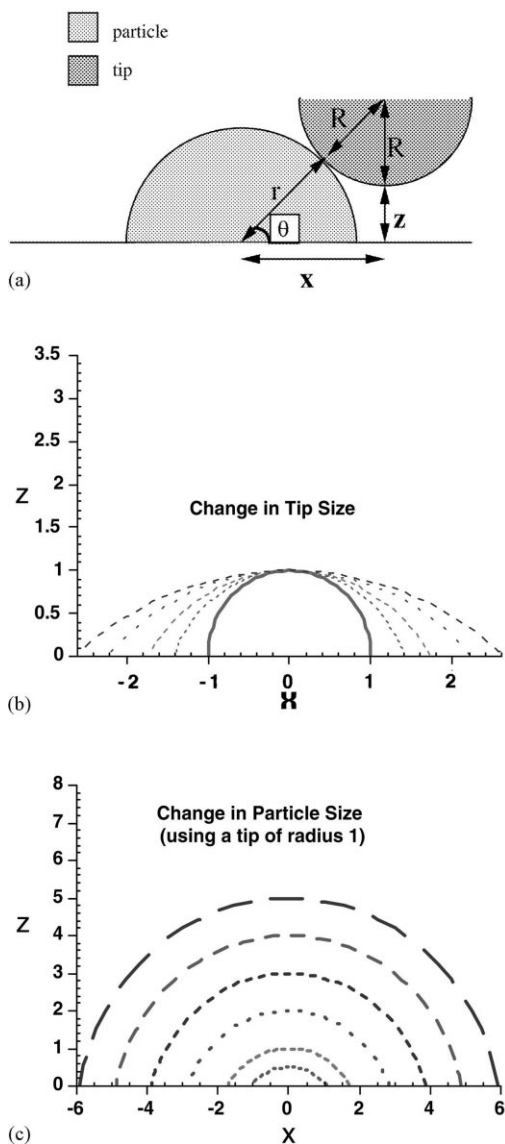


Fig. 3. Modelling of the effect of tip and particle size changes on the image obtained: (a) the geometric basis of the simple hemispherical model; (b) the effect of a change in tip size on the observed image for a hemispherical particle of unit radius (the smallest particle is the real size, while for the others the tip size was, in order of increasing apparent radius, 0.5, 1, 2, 3); (c) the effect of different particle sizes on the image obtained for a tip of unit radius (real particle sizes are 0.5, 1, 2, 3, 4, 5). In all these cases the height of the particle is determined, but the diameter depends on the relative sizes of tip and particle. For a small particle and large tip, the tip size is dominant, while a large particle and small tip combination gives reasonably accurate particle size determination. In all cases, the measured diameter is approximately an addition of the tip and particle diameters.

3. The importance of so-called precursor states for adsorption and catalysis

We can describe precursor states in the context of adsorption as any state which has a short lifetime on the surface, but through which long lifetime states are formed. Kisliuk first described the general kinetics associated with these kinds of states [5,6], and at the simplest level, this represents only a minor modification to the basic Langmuir idea of molecular adsorption, that is, the adsorption rate is given by

$$R_a = k_a(1 - \theta)$$

according to Kisliuk this becomes

$$R_a = k_a \left(1 + \frac{K\theta}{1 - \theta} \right)^{-1}$$

Although so simple, this form has a major modification for adsorption kinetics as shown in Fig. 5, helping keep the adsorption probability high during adsorption. This is because the precursor state parameter K is related to the ability of the precursor state to diffuse over a number of sites on the surface, thus, enabling it to 'seek-out' vacant sites for adsorption. This then explains some early observations of highly non-linear adsorption probability dependence on coverage [7–9], even some early observations by Langmuir himself [10], who had mentioned the possible involvement of diffusion of weakly held states in some adsorption processes. King went on to analyse adsorption systems in quantitative detail using these ideas [11], especially applied to nitrogen adsorption on W surfaces [12,13], and the reader is urged to refer to the aforementioned papers for a more complete description of the meaning and derivation of the precursor state parameter K .

Although weakly held, these states can be of fundamental importance in industrial catalysis. It may be that reaction rates are kept high on a catalyst with very few active sites by diffusion of molecules in such weakly held states. This may be of particular relevance to catalytic processes where there are a very limited number of active sites, e.g. metal catalysis with a high adsorbate steady state coverage, or catalysis on oxides which is dominated by defect sites at low concentration. In general, such states will play an important role for low temperature processes

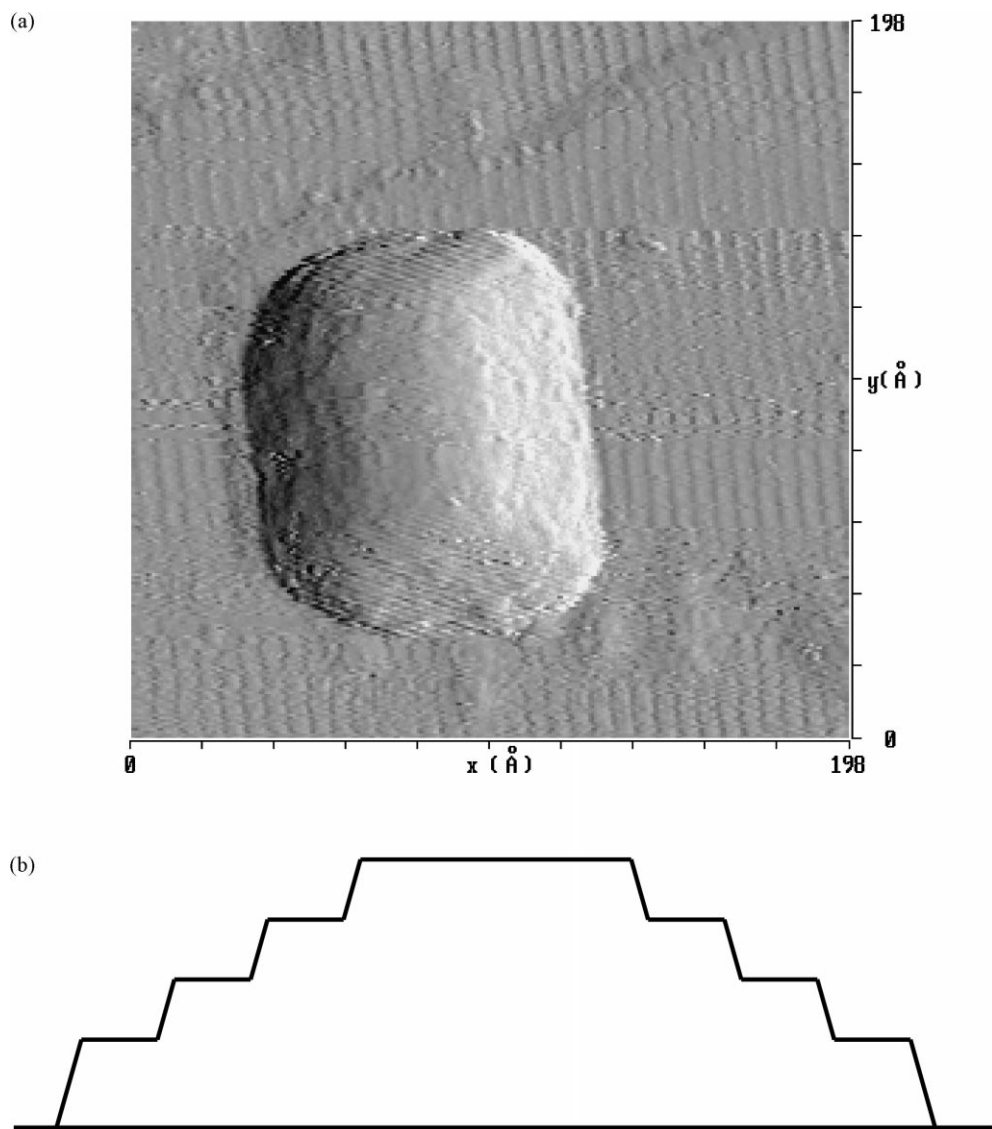


Fig. 4. (a) (Upper panel) image of a nano-ziggurat, the result of annealing a layer of 0.6 monolayers equivalent of Pd at 973 K for 15 min. Some details of this particle are imaged and steps are apparent on the side facets of the particle. Tunnelling at 1 nA, 0.5 V. (b) (Lower panel) a model of an ideal form of the ziggurat.

using moderately high molecular weight reactants (e.g. butene hydrogenation). For processes converting methane (low molecular weight, low heat of adsorption of molecular states, short surface lifetime), which occur at high temperature, the diffusion of such states is of correspondingly lower significance. Early work by Boudart involving hydrogen reaction

on glass surfaces already considered the importance of weakly held precursor states, as described in more detail below. These ideas incorporated the concept of the 'collection zone', and were extended to explain unusual observations regarding the oxidation of carbon monoxide on supported nanoparticulate catalysts.

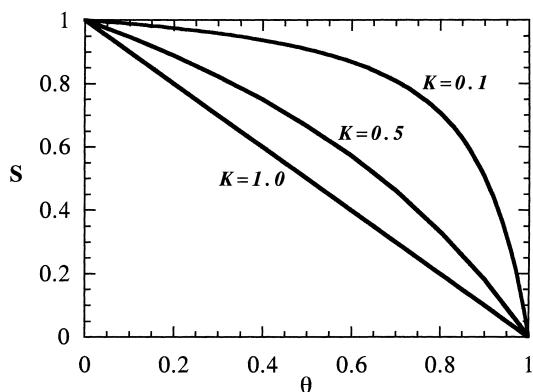


Fig. 5. Three adsorption curves of sticking probability against surface coverage using the Langmuir model for simple molecular adsorption ($K = 1$) and precursor-affected kinetics. The mobile precursor helps keep s high over a longer range of coverage; thus, at 0.8 monolayers coverage the precursor-mediated adsorption is four times as effective as for Langmuirian adsorption when $K = 0.1$.

4. Precursor state diffusion and the ‘collection zone’

Precursor state diffusion can be described in simplistic terms by so-called ‘diffusion circles’ [14] as

shown in Fig. 6. These show the area visited by a weakly held molecule on a surface simply as a circle containing the total number of hops, N_h , made by the molecule during its short sojourn on the surface. This is derived from the relative Frenkel lifetimes for desorption and diffusion in the following way:

$$N_h = \frac{\tau_d}{\tau_h} = \frac{A_d \exp(E_d/RT)}{A_h \exp(E_h/RT)}$$

The activation energy for hopping is very variable in relation to E_d , but a reasonable general estimate is that $E_h \sim E_d/3$. Thus, assuming similar A-factors, the average number of hops is given by

$$N_h \sim \exp\left(\frac{2E_d}{3RT}\right)$$

Of course, this is a trivial approach, but gives a nice idea of the extent of diffusion. Thus, the example in Fig. 6 is for a molecule with a heat of adsorption of 25 kJ mol^{-1} and shows that, even though the lifetime in the adsorbed state at the computed temperature of 300 K is very low (3 ns), the diffusive lifetime is much shorter enabling an average of 900 hops to be made in that time. In reality, there is not a sharp boundary

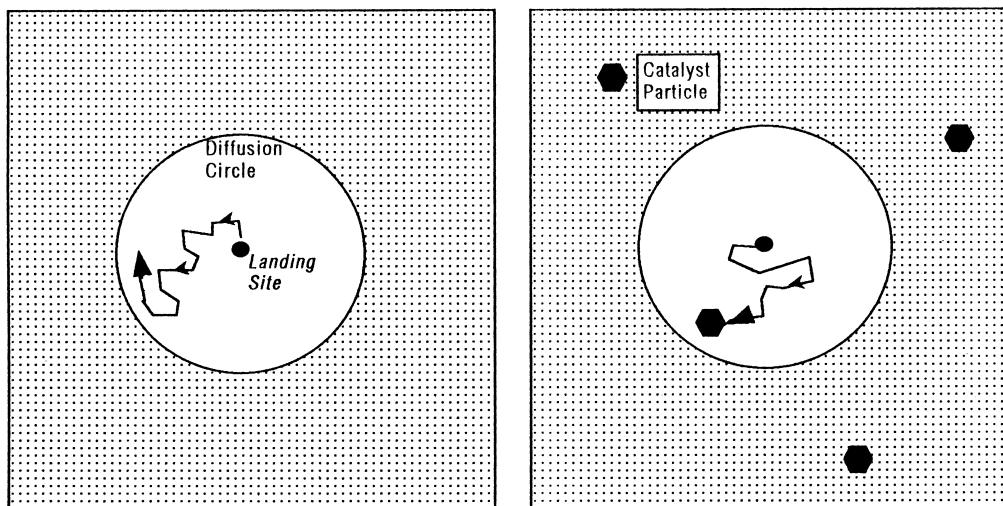


Fig. 6. Showing the diffusion circle concept for a mobile precursor on a square lattice with atomic positions indicated by dots. The left panel shows the approximate extent of diffusion of a precursor bound to the surface with 25 kJ mol^{-1} at 300 K; the diffusion circle extends 17 atomic sites from the landing site and approximately 900 sites are visited during the 3 ns sojourn on the surface. The right panel shows that this concept extends to the presence of active sites (catalyst particles) on an otherwise inactive surface; even though the particles are sparsely distributed the diffusion circle is so large that there is a high probability of a weakly held species finding such an active area. This is a similar concept to Boudart’s ‘collection zone’.

between sites visited and not visited; the probability of visitation simply declines away from the landing site and some sites will be visited at least twice.

In a series of papers [15–18], Boudart and co-workers have dealt with some aspects of this topic. In a ground-breaking paper, Tsu and Boudart [15] studied the recombination of hydrogen atoms impinging on glass surfaces and recognised the importance of the diffusion of weakly held, low coverage states of hydrogen atoms. They invoked the ‘collection zone’ concept to explain how these atoms were able to find reaction centres with higher probability than expected from their very low concentration on the surface. These ideas were revisited much later with similar, but more detailed work on SiO_2 [16], by Kim and Boudart. This approach was also applied to the results of studies of CO oxidation on a model $\text{Pd}/\text{Al}_2\text{O}_3$ catalyst, where the support was a single crystal of α -alumina. Boudart and co-workers [17,18] carried out careful work varying the particle sizes and surface density of the Pd nanoparticles, and found that the specific rate increased with decreasing particle size, and that for different number densities of similarly sized particles the specific rate was higher at lower Pd particle density. This was explained with reference to the earlier ‘collection zone’ model as due to reverse spillover of CO from the support to the active centre (the Pd particle). Thus, the flux to the active centre is enhanced by the presence of a collection zone region. The heat of adsorption of CO on the support was determined to be much higher than that of oxygen, being $\sim 28\text{kJ mol}^{-1}$, and although they considered this to be chemisorbed, it is certainly very weak and perhaps in the physisorbed state.

In elegant work which follows on from this Henry (who spent time in Boudart’s laboratory) carried out molecular beam measurements on model Pd catalysts in order to determine the sticking probability of CO on the surface [19]. The model catalyst consisted of Pd nanoparticles supported on single crystal $\text{MgO}(1\ 0\ 0)$. Henry et al. found that the bare support was inactive to chemisorption of CO, with an immeasurably low sticking coefficient into such a state. However, with Pd deposited at only 1% surface coverage, then the initial sticking coefficient was very high (close to unity). This was due to the reverse spillover of the weakly held CO, present in a short lifetime state on the support, from the collection zone region onto the

active Pd where the CO is strongly chemisorbed into a long lifetime state. Henry and colleagues have gone on to investigate a range of other systems, including the study of CO oxidation and other reactions, much of it being summarised in a recent review [20].

The diffusion circles shown in Fig. 6 above closely relate to this earlier concept of the collection zone, which was applied to adsorption and reaction on supported catalyst particles. If we imagine a catalyst particle as the centre of the diffusion circle shown in that figure then we have the collection zone as the diffusion circle. In effect, any molecule landing within the circle will have a high probability of finding the particle and adsorbing there. This then explains the observations of Henry. CO molecules landing on the MgO surface into a weakly held state of short lifetime will, nevertheless, diffuse to the Pd particles and adsorb there, providing they land within the collection zone, or that the distance to the nearest particle is less than the diffusion circle radius.

5. Spillover directly observed as it happens: oxygen storage and a new kind of SMSI

Spillover is a very important term in catalysis, having been originally coined by Khoobiar [21]. It is used as a shorthand description of the diffusion of adsorbed species from an active adsorbent to an otherwise inactive support. For instance, this could be diffusion of atoms from an active metal nanoparticle where dissociation is non-activated to a support where it is activated directly from the gas phase.

Using STM, we have recently identified oxygen spillover as it occurs from Pd nanoparticles to a $\text{TiO}_2(1\ 1\ 0)$ single crystal support [22,23]. Our STM is so stable at elevated temperatures that we have been able to record time-lapse ‘movies’ of such spillover at several temperatures [23]. It is important first, however, to understand what happens to the support in the presence of oxygen at elevated temperatures. Thus, Fig. 7 shows frames of the adsorption and reaction of oxygen with $\text{TiO}_2(1\ 1\ 0)$ occurring at 673 K. This shows that on the clean $\text{TiO}_2(1\ 1\ 0)$ surface, oxygen exposure results in the growth of new layers of TiO_2 ON TOP of the original surface [24,25]. How does this occur? It is known that treatment of TiO_2 to produce a good surface (involving Ar ion sputtering and thermal

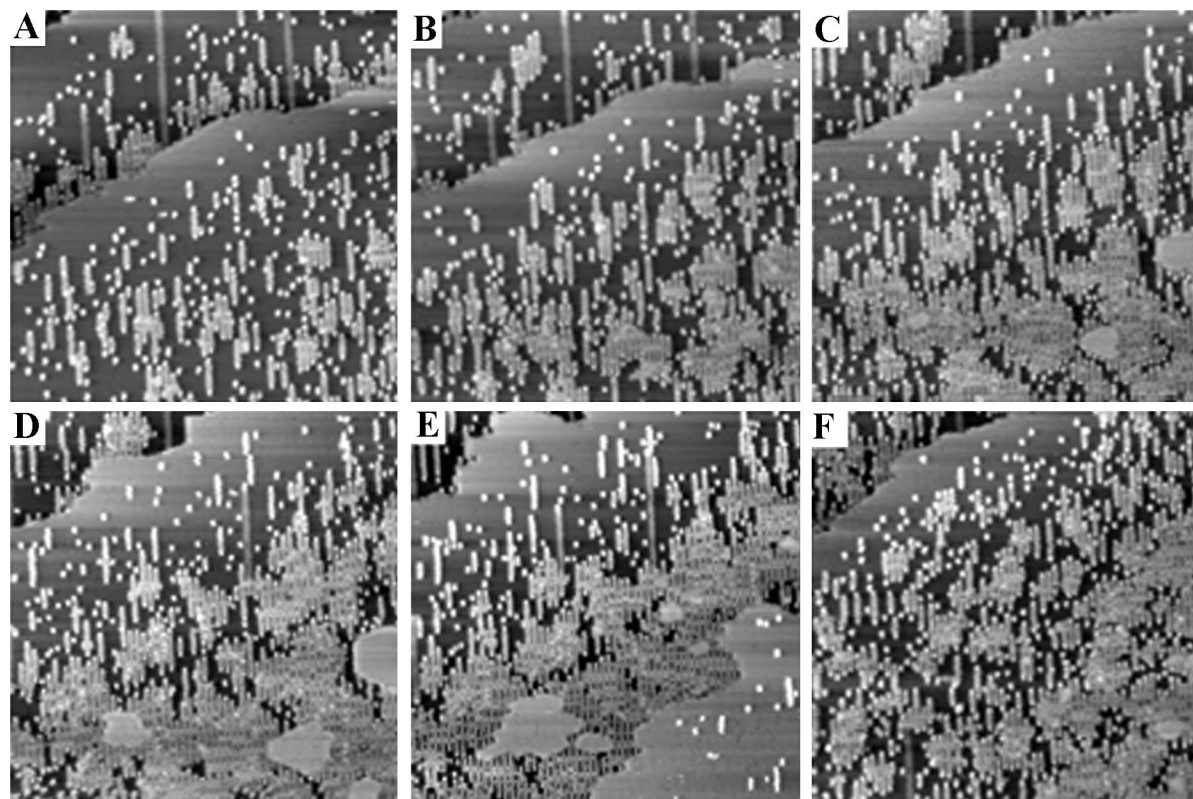


Fig. 7. A sequence of STM images taken at 673 K, showing re-oxidation of the $\text{TiO}_2(110)$ surface occurring by re-growth of TiO_2 layers at the surface. In panel A, a step edge can be seen running centre left to upper right, with nucleation (bright points) and growth (strings) of (1×2) areas on both upper and lower terraces. By panel C the step has advanced upwards and (1×1) islands are beginning to nucleate on the upper terrace (bottom right). In panels D, E these islands grow and coalesce, while the original step has now advanced to the top left of the image. In F, the (1×1) boundary at bottom right of panel E has advanced to the upper left, and that surface in turn is nearly covered by new (1×2) strings and islands. The oxygen pressure was 5×10^{-8} mbar, and tunnelling conditions were 0.1 nA, 1 V.

treatment) results in some reduction of the material (also seen in a colour change to blue). Even so, the level of non-stoichiometry is estimated to be very low at TiO_{2-x} where x is estimated to be $<10^{-3}$ in this work. Nevertheless, this then strongly affects how the surface reoxidises in an oxygen ambient at elevated temperature. We believe that the non-stoichiometry exists in the form of interstitial Ti^{3+} ions that are mobile through the lattice at elevated temperatures. They are probably in some kind of equilibrium with the surface, but are present in the bulk at very low steady-state concentration, and in dynamic flux. In the presence of oxygen gas they can become trapped at the surface where they grow new layers in a very particular fashion. They grow alternately new (1×2)

structured layers, which fill in to form the bulk (1×1) termination, again followed by a new layer of (1×2) and so on, in a cyclical fashion [24,25].

The question then arises as to what would happen in an oxygen ambient when nanoparticles are present on the surface? As illustrated in Fig. 8, will the particles float on the surface of the growing TiO_2 film, or will a pit be formed where the nanoparticle is, or will the growing TiO_2 layer encapsulate the nanoparticle? The equivalent experiment was carried out to that shown in Fig. 7, but now with Pd nanoparticles present on the surface, made by MVD. Fig. 9 shows such a surface before, during and after such a treatment. It is clear that several things happen here. Spillover of oxygen is seen to occur from the metal

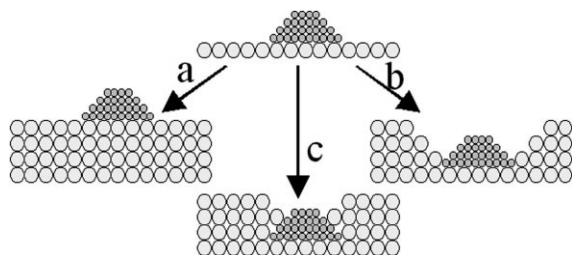


Fig. 8. Suggestions for what will happen to a Pd nanoparticle when the model catalyst is exposed to oxygen under similar conditions to those in Fig. 8. It may float on the growing TiO_2 layers (a), or a pit may form around the Pd particle, leaving it exposed to the vacuum (b), or it may become encapsulated (c), a kind of SMSI effect.

particle, which enhances the rate of oxygen adsorption (and hence, growth of new layers of TiO_2) adjacent to the Pd particles. This is the first time that spillover has been directly identified for an in situ reaction. The overall adsorption enhancement factor at 673 K is approximately a factor of 16 over the clean TiO_2 surface. The reason spillover occurs here is that the dissociation probability of oxygen on $\text{TiO}_2(110)$ is approximately 10^{-3} , whereas on Pd single crystals it is close to unity [26]. Thus, oxygen dissociates very efficiently on the Pd nanoparticles and is clearly able to diffuse onto the adjacent TiO_2 where the complex incorporation mechanism described above occurs. This leads to growth of new layers around the particle before layers are complete on the rest of the surface; in Fig. 9 seven layers of TiO_2 can be identified, by care-

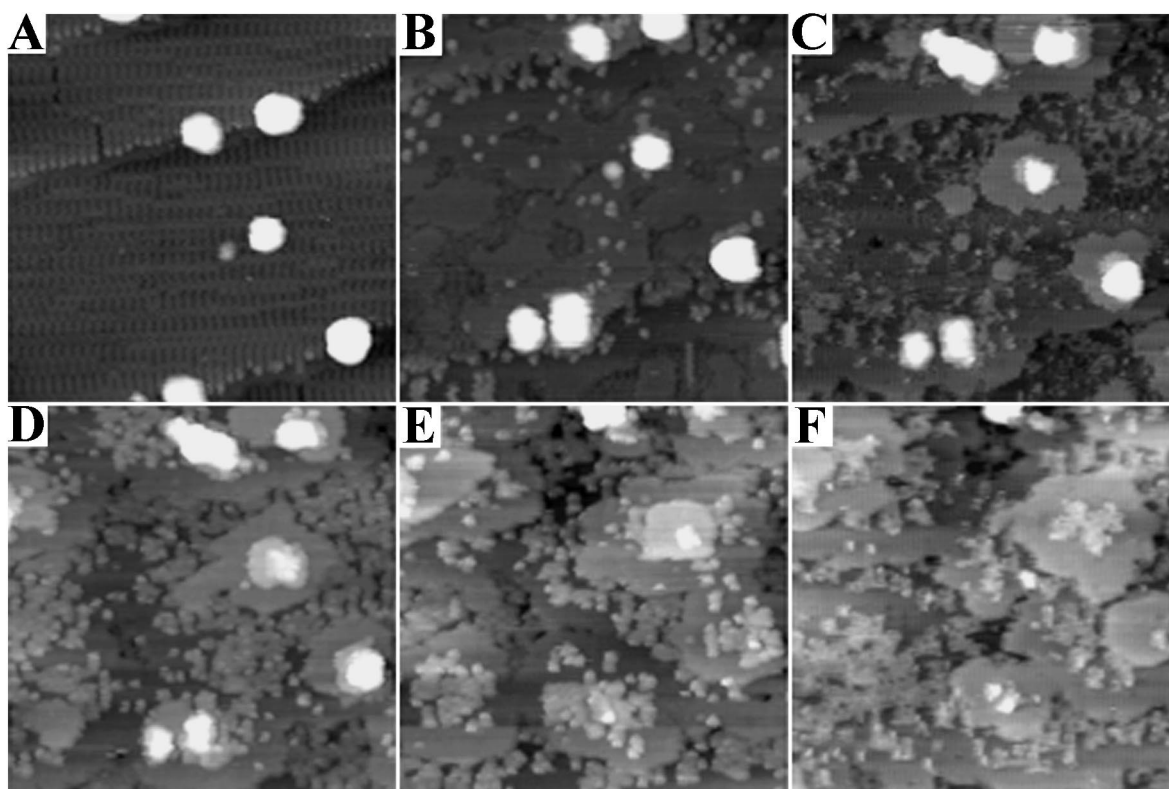


Fig. 9. A sequence of STM images taken at 673 K of oxygen spillover from Pd nanoparticles in an ambient pressure of 5×10^{-8} mbar of oxygen (doubled before image F). The total exposures to oxygen from image A–F were (in units of mbars): 114, 178, 237, 282, 344, 531. Note that there is an induction period before spillover is seen, probably due to build up of oxygen on the Pd particles. The spillover begins with the formation of one layer around the Pd particles, which then becomes multilayer growth, eventually burying the Pd particle with TiO_2 . In image F, a total of seven layers of TiO_2 have grown around the Pd on top of the original TiO_2 surface.

fully following the growth over a period of 155 min. The growth mechanism of these layers is also different from on the clean surface, always growing each layer in the (1×1) structure, rather than the alternat-

ing (1×1) and (1×2) growth described above. In this way layers build up around the particle like scaffolding, not as a single monolayer over the particle as often proposed for the classical SMSI effect seen in

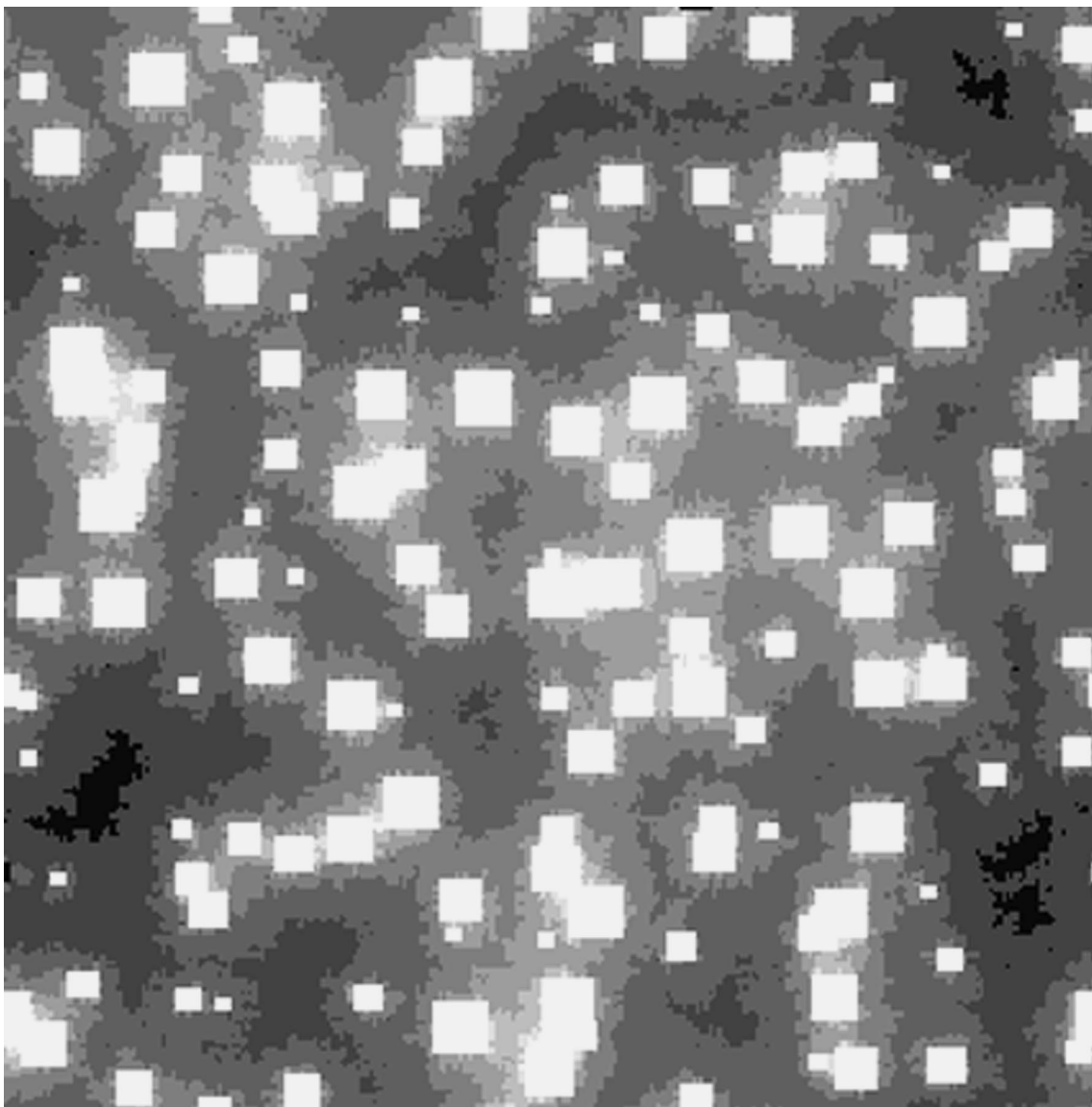


Fig. 10. Presenting a Monte Carlo simulation of O spillover on TiO_2 . Here the spillover process was simplified and simulated as a random walk of non-interacting atoms. The O source was considered to be the Pd particle. An initial site for starting random walk was chosen at random on top of a Pd particle. The random walk is performed on a square lattice, with the probability of jumping within an island or outside it being the same, however, it is forbidden for the atom to jump into an island from the outside. After every jump, if the atom lands on the external edge of a particle or island, it will have a probability of being trapped there of P (in this case $P = 0.01$). It is added to the island, and a new random walk event is started; otherwise the random walk continues until the atom is trapped elsewhere. The O coverage is equivalent to four monolayers. The O source was considered to be the Pd particle (shown as white squares).

catalysis after reduction treatments [27]. This reaction can be modelled to good effect, as shown in Fig. 10, using Monte Carlo methods. The main features of the spillover and SMSI processes are illustrated here and can be described by one simple probability parameter, namely the probability of trapping of oxygen at a step site (either the Pd–TiO₂ step, or that of the adjacent growing TiO₂ island itself). This is described in more detail in the figure legend.

This spillover effect is clearly an oxygen storage phenomenon. Oxygen is stored adjacent to the particle by conversion of interstitial Ti³⁺ to Ti⁴⁺. This is probably a close analogy to the oxygen storage function described for ceria in car catalysts where this process is proposed to work via the Ce⁴⁺/Ce³⁺ redox couple [28]. It should be possible to remove this oxygen again in a reducing environment, and to remove the Ti³⁺ so formed back into the interstitial sites.

6. Conclusions

In this paper, we have attempted to show the dramatic influence that STM, and other surface science techniques, is having on our understanding of basic phenomena and concepts in catalysis. We can now routinely fabricate nanoparticulate model supported catalysts which can be probed in ways not available to traditional catalysis.

Several concepts have been described:

1. Precursor states are shown to be very important for adsorption and catalysis. Diffusion in such weakly held states enables molecules to ‘seek-out’ active sites which may be sparsely distributed, and to find them with high probability, even though their lifetime may be very short on the surface. Further, they are responsible for the collection zone concept invoked by Boudart to explain higher than expected reaction rates for some surface reactions. They may also be the active species involved in reverse spillover phenomena generally.
2. Spillover has been observed for the first time in real-time and in situ. In this first case, oxygen is seen in STM to spill off Pd nanoparticles at 673 K onto the surrounding TiO₂ support surface where new layers of titania are built up around the Pd particles. This occurs by the conversion of subsurface interstitial Ti³⁺ ions to the oxide in a localised

manner. This type of oxygen incorporation is enhanced by the spillover by a factor of 16 compared to that in the absence of the nanoparticle. This is a kind of ‘Oxygen Storage’ phenomenon similar to that employed in car catalysis.

3. A kind of SMSI process has been identified, but occurring under oxidising conditions. In this case, the SMSI occurs by the build up of layers of growing TiO₂ around the Pd nanoparticles like scaffolding. In this way, the particles can eventually become totally encapsulated and deactivated for oxygen dissociation.

Acknowledgements

We are grateful for support for fellowships to RAB and AR from the EPSRC through grants GR/L22584 and GR/L13681 and to the University of Reading for the provision of a well-founded laboratory.

References

- [1] C.T. Campbell, Surf. Sci. Rep. 27 (1997) 1.
- [2] M. Valden, X. Lai, D.W. Goodman, Science 281 (1998) 1647.
- [3] A. Piednoin, E. Perrot, S. Granjeaud, A. Humbert, C. Chapon, C. Henry, Surf. Sci. 391 (1997) 19.
- [4] K. Hojrup Hansen, T. Worren, S. Stempel, E. Laegsgaard, M. Baumer, H.-J. Freund, F. Besenbacher, I. Stensgaard, Phys. Rev. Lett. 83 (1999) 4120.
- [5] P. Kisliuk, J. Phys. Chem. Solids 3 (1957) 95.
- [6] P. Kisliuk, J. Phys. Chem. Solids 5 (1958) 78.
- [7] G. Ehrlich, J. Chem. Phys. 34 (1961) 29.
- [8] D. Adams, L.H. Germer, Surf. Sci. 26 (1971) 109.
- [9] D. Adams, L.H. Germer, Surf. Sci. 27 (1971) 21.
- [10] J. Taylor, I. Langmuir, Phys. Rev. 44 (1933) 423.
- [11] D.A. King, CRC Crit. Rev. Solid St. Mater. Sci. 7 (1979) 167 and references therein.
- [12] D.A. King, M.G. Wells, Proc. R. Soc. Lond. A339 (1974) 245.
- [13] S.P. Singh-Boparai, M. Bowker, D.A. King, Surf. Sci. 53 (1975) 55.
- [14] M. Bowker, Surf. Rev. Lett. 1 (1994) 549.
- [15] K. Tsu, M. Boudart, 2nd Actes du Congres Int. de Cat. (Technip, Paris) 1 (1961) 593.
- [16] Y. Kim, M. Boudart, Langmuir 7 (1991) 2999.
- [17] F. Rumpf, H. Poppa, M. Boudart, Langmuir 4 (1988) 722.
- [18] L. Kieken, M. Boudart, in: Proceedings of the 10th International Congress of Catalysts, Budapest, Hungary, 1992.
- [19] C. Henry, C. Chapon, C. Duriez, J. Phys. Chem. 95 (1991) 700.
- [20] C.R. Henry, Surf. Sci. Rep. 31 (1998) 231.

- [21] S. Khoobiar, *J. Phys. Chem.* 68 (1964) 411.
- [22] R.A. Bennett, P. Stone, M. Bowker, *Catal. Lett.* 59 (1999) 99.
- [23] R.A. Bennett, P. Stone, M. Bowker, *Faraday Disc.* 114 (1999) 267.
- [24] R.A. Bennett, P. Stone, N. Price, M. Bowker, *Phys. Rev. Lett.* 82 (1999) 3831.
- [25] P. Stone, R.A. Bennett, M. Bowker, *New J. Phys.* 1 (1999) 8 (www.njp.org).
- [26] I.Z. Jones, R.A. Bennett, M. Bowker, *Surf. Sci.* 439 (1999) 235.
- [27] S. Tauster, *Acc. Chem. Res.* 20 (1987) 389.
- [28] B. Harrison, A. Diwell, C. Hallett, *Plat. Met. Rev.* 32 (1988) 73.